Waterside Corrosion in Zirconium Alloys

Arthur T. Motta

The influence of the alloy microstructure and microchemistry on uniform waterside corrosion of zirconium alloys is reviewed, with special attention to the various stages of corrosion, such as pre-transition, transition, and breakaway.

INTRODUCTION

Zirconium alloys have been used for more than 50 years as nuclear reactor fuel cladding.[1] Corrosion of Zr alloy fuel cladding by the reactor coolant water and the associated hydrogen pickup is a potential life-limiting degradation mechanism for nuclear fuel.[2] In particular, the acceleration of corrosion with continuing reactor exposure is one of the potential limiting factors in attempting to increase fuel burnup in current and future reactors.[3–5]

Zirconium alloys have been chosen for nuclear fuel cladding because of their low neutron absorption cross-section, good resistance to high temperature corrosion, adequate mechanical properties, and resistance to radiation damage. The resistance of Zr alloys to waterside corrosion (defined here as uniform corrosion by coolant water, as opposed to inner-diameter stress corrosion cracking or to localized forms of corrosion such as nodular corrosion) originates from the protective oxide formed on its surface and which hampers further corrosion.[6,7] Pure Zr tends to grow an unstable oxide which is very susceptible to breakaway,[8] but small additions of alloying elements, such as Sn, Fe, Cr, and Ni present in Zircaloy-2 and/or Zircaloy-4 cause the oxide formed to be protective and stable.[8,9] Zirconium alloy fabrication, chemical composition, and microstructure have been optimized over the years to yield the best possible corrosion and hydrogen pickup behavior,[1] since a clear effect of the alloy on corrosion rate has been shown.[10] Considerable performance improvements have been achieved over the years through systematic empirical studies to optimize corrosion resistance of these and other alloys.[4,11–13] However, the fundamental reasons why such procedures yield the best results are still not well known.

It is clear that the combination of alloy composition and thermo-mechanical treatment of the alloy (and thus the alloy microstructure) significantly affects the corrosion process in Zr alloys.[14] Associated with corrosion is the issue of hydrogen pickup: a fraction of the hydrogen generated in the corrosion reaction is absorbed by the sample and is commonly referred to as the hydrogen pickup fraction.[15] Hydrogen forms brittle hydrides in the alloy which can significantly degrade cladding ductility.[16–18] Generally the amount of hydrogen absorbed by the material increases with oxide thickness, but for a given thickness, different alloys can show different hydrogen pickup fractions.[7] It is thus of interest to fuel vendors and utilities to understand the mechanisms of formation of a stable protective oxide, the mechanisms of oxide transition and susceptibility of the alloy to undergo breakaway corrosion so as to minimize hydrogen pickup and associated embrittlement.

This article will focus on studies to discern the relationship between alloy composition and microstructure and corrosion behavior. Because of the complexity of the issues, the focus is on laboratory-based autoclave corrosion, while recognizing that in-pile corrosion rates are different—and normally higher—than those obtained in the laboratory. Nevertheless, autoclave

How would you…

…describe the overall significance of this paper?

The paper presents the state of the knowledge on uniform corrosion of zirconium alloys in nuclear power plants, focusing especially on the influence of the alloy chemical composition and microstructure. Zirconium alloys with slightly different composition and microstructure show widely different corrosion behavior. Such differences are manifested in the corrosion rate in the region of protective oxide growth and on the oxide transition, and are likely caused by differences in oxide microstructure, the investigation of which with state of the art techniques can yield insights on the mechanisms of alloy protectiveness and lead to the design of better alloys.

…describe this work to a materials science and engineering professional with no experience in your technical specialty?

Different zirconium alloys used for nuclear fuel cladding experience widely different corrosion rates and incidence of oxide breakaway. This article explores the mechanistic reasons for this difference in terms of the corrosion rate in the protective regime and in terms of determining the time to oxide transition or breakaway. The understanding of these processes can lead to the design of better alloys that can withstand longer exposures in the reactor leading to more economical and safe exploitation of nuclear power.

…describe this work to a layperson?

Nuclear fuel encased in zirconium alloy tubular cladding is immersed in coolant water when operating in a nuclear reactor. In this environment, corrosion of the tubing in the coolant water can lead to tubing failure. This article discusses the influence of the alloy used on the corrosion process and points to outstanding questions that if resolved could lead to better alloy design.

corrosion testing has been found to correlate well with in-pile behavior, in that alloys that behave well in autoclave testing normally also behave well in reactor.

See the sidebar for Zr alloy corrosion kinetics.

UNDERSTANDING CORROSION BEHAVIOR

Figure A suggests that we can understand corrosion behavior by individually understanding the pre-transition behavior, the onset of transition and the tendency for the onset of breakaway.

Pre-transition Behavior

In the pre-transition regime the barrier layer is the intact part of the oxide layer that serves as an obstacle to the ingress of oxidizing species.[28] In any corrosion process the overall corrosion rate is determined by the rate of the slowest step, that is, the rate-limiting step. In the case of corrosion in the pre-transition regime, since the corrosion rate decreases with increasing oxide thickness, the rate-limiting step should be the transport of oxidizing species through the barrier layer, rather than a surface reaction.[29] It has been well documented that the Zr ions do not migrate through the oxide layer and that corrosion occurs by ingress of oxygen ions only. Thus, the pre-transition kinetics are determined by the migration of oxygen atoms (and the reverse flux of vacancies) through the oxide barrier layer, either through the bulk or through the oxide grain boundaries.[30] Electric neutrality is maintained by electron transport or hydrogen ingress through the oxide layer.

When the migration of oxygen atoms is rate-determining and occurs through a homogenous, uncracked oxide, we obtain parabolic kinetics (n=0.5 in Equation 1). When the most corrosion kinetics observed are sub-parabolic, some process must slow the overall rate of corrosion[31] relative to that of parabolic behavior. Many possible mechanisms for such slow down have been proposed, from the development of lateral cracks that impede diffusion, to increasing grain size that reduces the available area for migration, to the role of stress in hampering diffusion.[32,33] The most likely scenario is that the transport of electrons in the oxide layer (or the ingress of H atoms) necessary to close the reaction circuit can become the rate limiting step for corrosion. That is, when the oxide thickness grows, the electron transport may become slower than oxygen transport (and thus rate-limiting), and corrosion kinetics slow to maintain electric neutrality.[32]

Detailed measurements of the pre-transition kinetics have shown that the value of n varies with the alloy. In general, Zr-Nb alloys exhibit corrosion kinetics that are close to parabolic, while Zircaloy-4 shows sub-cubic kinetics

ZIRCONIUM ALLOY CORROSION KINETICS

Zirconium oxide is observed in two principal variants, tetragonal and monoclinic oxide, the latter being the stable phase at 360°C. The tetragonal phase is stabilized by stress, by sub-stoichiometry, by small grain size and by alloying elements, all of which are present in the growing oxide.[19–21] In most cases, however, the growing oxide is predominately monoclinic, although the tetragonal fraction can vary depending on the alloy and on the stage of corrosion as discussed below.

The corrosion kinetics of zirconium alloys exposed to high temperature (360°C) water varies widely from alloy to alloy, as shown in Figure Aa.[22,23] As shown by the black lozenge points, Zircaloy-4 shows an initially fast corrosion layer increase which slows down as the layer thickness grows. In this regime the corrosion thickness δ is normally well described by an equation of the form

$$\delta = At^n \quad (1)$$

where A and n are constants and t is the exposure time. Values of n range from 0.2 to 0.5 during corrosion in 360°C pure water.[24] At a given thickness, the corrosion rate abruptly increases, reverting to the value observed at the start of the oxidation, indicating a loss of protectiveness of the oxide layer. This is called the oxide transition.[6] The corrosion process then resumes at the same rate as before the transition, and the process repeats itself continuously at constant intervals. In fact, one of the notable facts about zirconium alloy corrosion is that the transition thickness is remarkably reproducible for a given alloy and a given corrosion condition.[23] These transitions appear also to be remarkably constant during corrosion, that is, the n^{th} cycle is similar to the first. Figure Ab shows transmitted light optical microscopy pictures of corrosion layers in Zircaloy-4, in which 17 evenly spaced transitions can be seen, while ZIRLO exhibits a similar regular pattern, a little more widely spaced.[25] The other curves in Figure Aa illustrate the range of corrosion behavior exhibited by different model zirconium alloys. Some alloys do not show recovery when transition occurs and go into breakaway (Zr-1.0Cr-0.2Fe). Normally, once breakaway sets in, the oxide does not recover. Other alloys never exhibit protective behavior in the first place, and go immediately into breakaway (Zr-0.5Cr in Figure Aa).[26] We should note that varying the range of oxygen and hydrogen pressure in the water over a wide range has little effect on the corrosion behavior, although dissolved ions such as Li can have a strong deleterious effect on corrosion.[27]

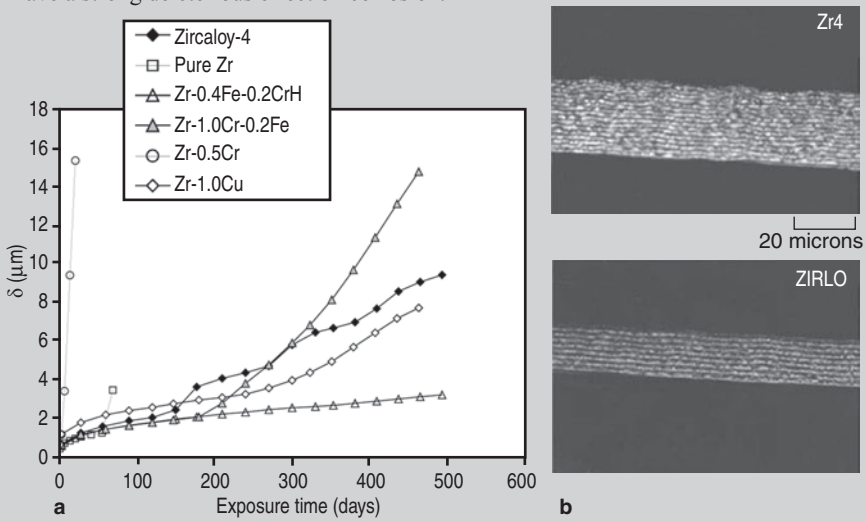

Figure A. (a) Corrosion film thickness as a function of exposure time in 360°C pure water for various zirconium alloys as indicated;[51] (b) transmitted light optical micrographs of oxide layers formed in Zircaloy-4 and in ZIRLO showing the periodic layers associated with successive oxide transitions formed during corrosion.[23]

(n=0.2–0.25).[24] Presumably this difference arises from different microstructure and micro-chemistry among the different alloys.

One of the outstanding questions is how does the microstructure differences present in these alloys (different distributions of alloying elements in the matrix or in precipitates) affect the corrosion kinetics as they do. The observation that different alloys corrode at different rates in the same autoclave indicates that it is likely that the differences in corrosion behavior arise from different oxide microstructures that form as a result of different alloy microstructures. Specific oxide microstructures have been associated with protective behavior.[23,25,34] The connection between alloy microstructure and oxide microstructure has not been established yet, however.

The Oxide Transition

The corrosion of Zr alloys that exhibit stable oxide growth is often characterized by the repetitive growth of oxide layers of constant thickness. At a critical layer thickness, a transition to the growth of a new layer begins and the process continues. This layered oxide structure has been observed in both autoclave and in-reactor specimens.[35,36]

Different mechanisms have been proposed to explain the loss of protectiveness in the oxide layer observed at the oxide transition, with two in particular receiving the greatest attention: percolation of porosity[37] and stress accumulation and mechanical breakup of oxide.[38] It is well known that porosity, in the form of small intergranular tubular channels develops in growing oxide layers.[39,40] The percolation of such porosity from the water oxide interface to the oxide metal interface could provide an easy path for the access of water to the base metal,[39,41,42] but it is not clear why different materials would consistently exhibit different porosity formation rates. The second possibility is that stresses accumulate in the oxide layer such that when a critical level is reached oxide mechanical breakup occurs, thus creating cracks that allow easy ingress of water to the interface. Evidence for stress accumulation in growing oxide films supports this hypothesis.[43–45] The stresses that accumulate in the oxide are in-plane stresses which would cause lateral (rather than vertical) cracking. In fact only horizontal cracks are commonly observed in post-transition oxides. These horizontal cracks normally would not result in easy access of water to the underlying metal.[34]

The hypothesis is then that different alloys form oxide layers that accumulate stress at different rates as they grow. One possibility is that a combination of the two is responsible for the transition. That is, porosity gradually develops, possibly at an equal rate for all alloys, but oxides break up at different thicknesses. When the oxide breaks up as a result of accumulated stress the cracks thus created connect the existing pores. This produces a sudden percolation of porosity that allows easy access of water to the metal. The remarkable reproducibility of the transition thickness occurs because stresses accumulate at a characteristic rate for a given alloy, such that mechanical failure (transition) occurs at a constant oxide thickness.[24] The question still remains as to what causes stress to accumulate differently in different alloys. Stress accumulation occurs as a result of the volume change (56%) associated with the transformation of Zr into ZrO_2.[46] Although most of this volume change is accommodated in the vertical (oxide growth) direction, even a small deviation from a perfect accommodation of these transformation strains would cause significant stress to accumulate.[47]

At the oxide transition, many of the conditions that stabilize the tetragonal phase disappear and the tetragonal phase content decreases.[25,48] Because of this, the tetragonal phase has often been correlated with protective behavior and the monoclinic phase with non-protective behavior. However, tetragonal phase content is likely an effect rather than a cause of corrosion behavior, as alloys with lower tetragonal phase content in the pre-transition regime have later transitions than alloys with higher tetragonal phase content.[23]

Breakaway

A disruption in the repetitive growth process can result in the onset of breakaway corrosion which is characterized by the absence of regular transitions and fast, non-saturating oxide growth. This unstable (breakaway) oxide growth has been observed during both autoclave testing (e.g., testing in lithiated water or testing of hydrogen-charged specimens) and during reactor exposure.

The reasons for corrosion breakaway are not well known. During reactor exposure the formation of a hydride rim at high burnup has been identified as a possible cause of higher corrosion rates observed in-reactor after 40–50 GWd/ton.[3] The hydride rim does not form in autoclave corrosion, however, because no temperature gradient exists to induce preferential hydride precipitation at the outer rim, and the cause of breakaway has to be sought elsewhere.

Breakaway is characterized by unstable oxide growth. The fact that once breakaway starts it keeps going means the oxide microstructure induces unstable oxide growth. Therefore, a reasonable path is to compare the oxide-metal interface of oxides that have undergone breakaway to that of protective oxides. Synchrotron radiation diffraction and fluorescence examination of breakaway oxide layers and protective layers shows marked differences between stable and non-stable oxide layers.

PROTECTIVE OXIDE CHARACTERISTICS AND CORROSION MECHANISM

Protective oxides formed on Zr alloys during autoclave corrosion show particular common characteristics, which are now beginning to be understood. In particular, protective oxides show intermediate phases at the oxide-metal interface that are associated with stable growth. Figure 1 shows a succession of diffraction patterns taken from an oxide layer formed on ZIRLO during autoclave corrosion in 360°C water. The diffraction patterns were obtained using microbeam synchrotron radiation diffraction and fluorescence, in which a 0.2 micron x-ray beam is scanned across the oxide, generating successive plots of diffracted intensity versus two-theta angle. The diffraction peaks observed can be indexed to identify the phases present as a function of position in the oxide layer (Figure 1).

In the metal side of the plot, intense alpha-Zr peaks are clearly seen

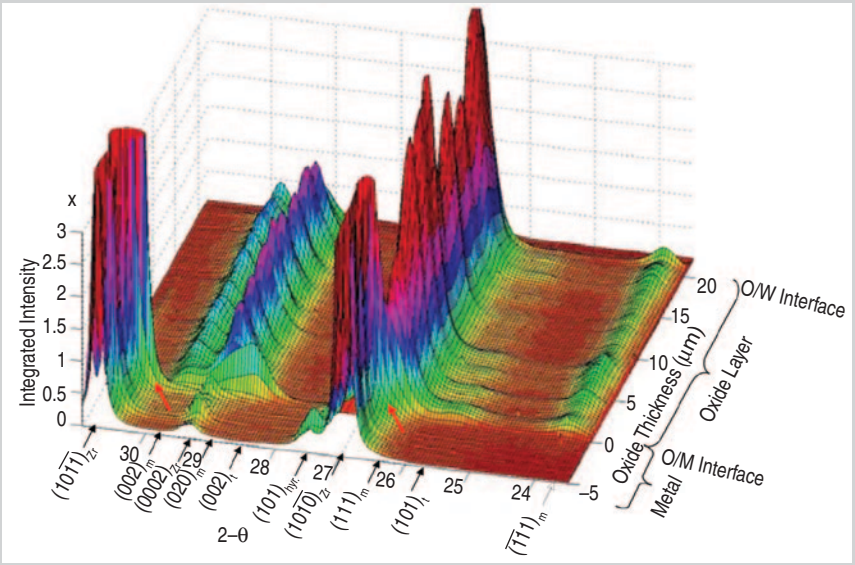

Figure 1. X-ray diffracted intensity versus two-theta angle, scanned across the oxide layer thickness, of ZIRLO oxide layer formed after exposure to 360°C pure water for 784 days. The peaks associated with various phases present in a protective oxide, especially near the oxide-metal interface, are shown.[23]

(cropped). When the metal side near the oxide metal interface is examined in more detail, peaks belonging to a suboxide phase Zr_3O, are observed and this phase is normally present in protective oxides. When the oxide-metal interface is tranversed, peaks belonging to the monoclinic ZrO_2 phase (hkl_m) become quite evident, as identified in the plot. The overall monoclinic oxide orientation has the $(200)_m$ plane parallel to the oxide-metal interface.[45,49] In the cross section geometry used this means the $(200)_m$ intensity is close to zero. (In the figure we use the notation $(hkl)_X$ to designate the (hkl) plane of phase X.)

Observing more closely, we note periodic oscillations in several of the monoclinic and tetragonal peaks. The oscillations in the peaks mentioned above match very well with the periodic transitions visible in the oxide thickness plot such as shown in Figure Aa, indicating that they are related to the oxide transitions. Figure 2 shows the diffracted intensities for the $(020)_m$ and the $(101)_t$ peaks. The regular oscillations correspond well both with the periods seen in the oxide thickness and with the regular periods seen in Figure Ab. Interestingly, the tetragonal and monoclinic are seen be out of phase with each other, indicating that at certain times the tetragonal phase forms preferentially to the monoclinic.

Transmission electron microscopy observations of the oxide layer have shown that protective oxide growth is associated with the formation of well-oriented columnar grains. The columnar monoclinic oxide formed on Zr alloys is highly textured, exhibiting a fiber texture with the $(200)_m$ plane parallel to the oxide-metal interface.[49] This is true of both protective and non-protective oxide layers. However, the more protective oxide layers show particular micro texture characteristics. In particular the protective oxides show wider columnar grains, with smaller grain-to-grain mis-orientations than the non-protective oxides.[34] This is understood in the context of easier porosity formation in highly mis-oriented grain boundaries.

In addition near the oxide-metal interface a different structure is observed than in the middle of the oxide layer. In particular a highly oriented tetragonal phase is observed which is a precursor of the main monoclinic phase. This highly oriented tetragonal phase has been consistently observed in protective oxides both in 360°C corrosion and during corrosion in 500°C supercritical water[50] and is not observed in non-protective breakaway oxides. An orientation relationship has been determined of

$$(10\bar{1}0)Zr \,//\, (002)t \,//\, (020)m \qquad (2)$$

Thus, the highly oriented tetragonal phase is a precursor phase that helps induce well-oriented in-plane orientation of the growth of the monoclinic phase leading to less stress accumulation and porosity development which in turn leads to a delayed transition.

Mechanism of Oxide Growth

From the ensemble of the observations above, the following mechanism of oxide growth was proposed that is in agreement with experimental evidence.[24,25] At the beginning of the oxidation small oxide grains nucleate with a comparatively high percentage of tetragonal grains because of the stabilization of the tetragonal phase relative to monoclinic afforded by the small grain size (possibly aided by high stress and oxide sub-stoichiometry). Some of these small grains are properly oriented for growth (they have their (110)t or $(1\bar{1}0)t$ planes parallel to the oxide-metal interface.) As these grains grow, they become columnar and when they pass the critical diameter of ~30 nm column length they transform to mono-

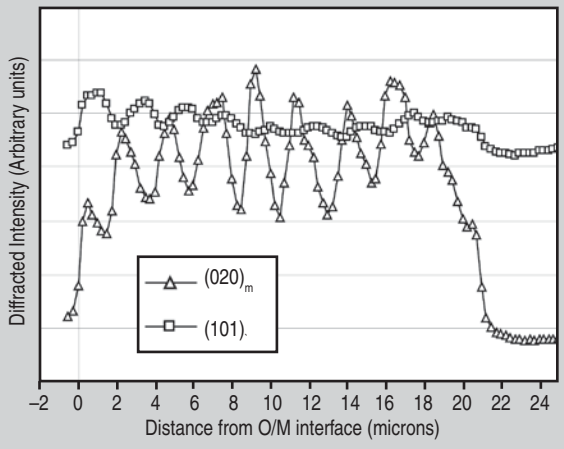

Figure 2. Periodic variations in diffracted intensity for the $(020)_m$ and $(101)_t$ peaks as a function of distance from the oxide-metal interface in ZIRLO corroded in 360°C water for 784 days.[23]

clinic oxide, maintaining the same orientation. The improperly oriented tetragonal grains never grow and remain as small tetragonal grains embedded in the oxide. The monoclinic columnar grains, properly oriented with $(200)_m$ near the oxide-growth direction, grow into the metal. When these grains reach aspect ratios of 4 to 5, small mismatches in crystalline orientation relative to the preferred orientation cause the columnar grains to stop growing and induce renucleation at the leading edge of the grain. When renucleation occurs at the end of the grain, the freshly created small equiaxed grains have a higher percentage of tetragonal phase, and thus in that location a high tetragonal fraction is observed. Because larger columnar grains have to renucleate less frequently the tetragonal fraction is lower in large-grained oxides in pure water.

On the scale of the overall oxide thickness, stresses accumulate in the bulk of the oxide eventually causing the oxide to crack, and to create the percolation condition which causes the oxide transition. Upon transition, a global renucleation of the oxide grains occurs with a greater percentage of tetragonal phase, thus causing a greater tetragonal intensity to be observed. It is still not clear what the specific role of the alloying elements and alloy microstructure is in promoting the oxide microstructures that lead to stable oxide growth, but research is ongoing to discern these causes.

CONCLUSION

Although many advances have been made in recent years, much progress still needs to be made to understand mechanisms of alloy protection and thus be able to design better alloys.

References

1. C. Lemaignan and A. T. Motta, *Materials Science and Technology, A Comprehensive Treatment*, vol. 10B, ed. B.R.T. Frost (New York: Wiley-VCH, 1994), pp. 1–51.
2. R. Yang, O. Ozer, and H. Rosenbaum, "Current Challenges and Expectations of High Performance Fuel for the Millennium" (Paper presented at the Light Water Reactor Fuel Performance Meeting, Park City, Utah, ANS, 2000).
3. M. Blat, L. Legras, D. Noel, and H. Amanrich, *Twelfth Int.l Symp. on Zr in the Nuclear Industry*, STP 1354 (West Conshohocken, PA: ASTM, 2000), pp. 563–591.
4. P. Bossis, D. Pecheur, K. Hanifi, J. Thomazet, and M. Blat, *J. ASTM Int.,* 3 (2006) paper #JAI12404.
5. G. Zhou, G. Wikmark, L. Hallstadius, J. Wright, M. Dahlback, L.P. Brandes, S. Holcombe, U. Wetterholm, A. Lindquist, S. Valizadeh, Y. Long, and P. Blair, *Proceedings of Top Fuel 2009* (Paris: American Nuclear Sociey, 2009), paper 2020.
6. B. Cox, *J. Nuclear Materials,* 336 (2005), pp. 331–368.
7. "Corrosion of Zirconium Alloys in Nuclear Power Plants," Doc. No IAEA-TECDOC-684 (Vienna, Austria: International Atomic Energy Agency, 1993).
8. "Waterside Corrosion of Zirconium Alloys in Nuclear Power Plants," Doc. No IAEA-TECDOC-996 (Vienna, Austria: International Atomic Energy Agency, 1998).
9. E. Hillner, *Proc. 3rd Int. Symp. on Zr in the Nuclear Industry*, ASTM STP 633 (1977), pp. 211–235.
10. S. Kass, *Proc. Symp. on Corrosion of Zirconium Alloys,* ASTM, STP 368 (La Grange Park, IL: American Nuclear Society, 1964), pp. 3–27.
11. G.P. Sabol, G.R. Kilp, M.G. Balfour, and E. Roberts, *Eighth Int. Symp. on Zirconium in the Nuclear Industry*, ASTM STP 1023 (West Conshohocken, PA:, ASTM, 1989), pp. 227–244.
12. G.L. Garner and J.P. Mardon, *Nuclear Engineering Int.,* 47 (2002), pp. 36–37.
13. J.P. Mardon, D. Charquet, and J. Senevat, *12th Int. Symp. on Zr in the Nuclear Industry,* ASTM STP 1354 (West Conshohocken, PA:, ASTM, 2000), pp. 505–524.
14. F. Garzarolli and H. Stehle, *IAEA Symp. on Improvements in Water Reactor Fuel Technology and Utilization*, SM 288/24 (Vienna, Austria,; IAEA, 1986), pp. 387–407.
15. N. Ramasubramanian, P. Billot, and S. Yagnik, "Hydrogen Evolution and Pickup during the Corrosion of Zirconium Alloys: A Critical Evaluation of the Solid State and Porous Oxide Electrochemistry," *ASTM Special Technical Publication 1423* (West Conshohocken, PA: ASTM, 2002), pp. 222–242.
16. D.L. Douglass, *The Metallurgy of Zirconium* (Vienna, Austria: International Atomic Energy Agency Supplement, 1971).
17. J.B. Bai, C. Prioul, and D. Francois, *Metall. Mater. Trans. A,* 25A (1994), pp. 1185–1197.
18. C.E. Ells, *J. Nuclear Mater.,* 28 (1968), pp. 129–151.
19. R.C. Garvie, *J. Phys. Chem.,* 69 (1965), pp. 1238–1243.
20. R.C. Garvie, *J. Phys. Chem.,* 82 (1978), pp. 218–224.
21. J. Godlewski, *10th Int. Symp. on Zr in the Nuclear Industry*, ASTM STP 1245 (West Conshohocken, PA: ASTM, 1994), pp. 663–686.
22. A. Yilmazbayhan, "Microstructural Basis of Uniform Corrosion in Zr Alloys" (Ph.D Thesis in Nuclear Engineering, Penn State University, 2004).
23. A. Yilmazbayhan, A.T. Motta, R.J. Comstock, G.P. Sabol, B. Lai, and Z. Cai, *J. Nuclear Materials,* 324 (2004), pp. 6–22.
24. A.T. Motta, M.J. Gomes-da-Silva, A. Yilmazbayhan, R.J. Comstock, Z. Cai, and B. Lai, *J. ASTM International,* 5 (2008), paper ID# JAI10125.
25. A.T. Motta, A. Yilmazbayhan, R.J. Comstock, J. Partezana, G.P. Sabol, Z. Cai, and B. Lai, *J. ASTM International,* 2 (2005), Paper # JAI 12375.
26. A. Yilmazbayhan, A.T. Motta, H.G. Kim, Y.H. Jeong, J.Y. Park, and R. Comstock, *Environmental Degradation of Materials in Nuclear Power Systems XII*, ed. L. Nelson, P.J. King and T.R. Allen (Warrendale, PA: TMS, 2007), pp. 201–210.
27. D. Pecheur, J. Godlewski, P. Billot, and J. Thomazet, *11th Int. Symp. on Zr in the Nuclear Industry*, ASTM STP 1295 (West Conshohocken, PA: ASTM, 1995), pp. 94–113.
28. P. Barberis and A. Frichet, *J. Nuclear Materials,* 273 (1999), pp. 182–191.
29. B. Cox, *J. Corrosion Science and Eng.,* 6 (2003), paper 14.
30. B. Cox and J.P. Pemsler, *J. Nuclear Mater.,* 28 (1968), pp. 73–78.
31. M. Tupin, M. Pijolat, F. Valdivieso, M. Soustelle, A. Frichet, and P. Barberis, *J. Nuclear Mater.,* 317 (2003), pp. 130–144.
32. A.T.J. Fromhold, *Theory of Metal Oxidation,* vol. 9 (New York: North-Holland, 1976).
33. G.P. Sabol and S.B. Dalgaard, *J. Electrochemical Soc.,* 122 (1975), p. 316.
34. A. Yilmazbayhan, E. Breval, A. Motta, and R. Comstock, *J. Nuclear Mater.,* 349 (2006), pp. 265–281.
35. P. Bossis, G. Lelievre, P. Barberis, X. Iltis, and F. Lefebvre, *Twelfth Int. Symp. on Zirconium in the Nuclear Industry*, ASTM STP 1354 (West Conshohocken, PA: ASTM, 2000), p. 918.
36. P. Bossis, F. Lefebvre, P. Barberis, and A. Galerie, *Materials Science Forum,* 369-372 (2001), pp. 255–262.
37. B. Cox, *J. Nuclear Mater.,* 29 (1969), p. 50.
38. D.H. Bradhurst and P.M. Heuer, *J. Nuclear Mater.,* 37 (1970), p. 35.
39. B. Cox, *J. Nuclear Mater.,* 27 (1968), pp. 1–11.
40. N. Ni, S. Lozano-Perez, M.L. Jenkins, C. English, G.D.W. Smith, J.M. Sykes, and C.R.M. Grovenor, *Scripta Materialia,* 62 (2010), pp. 564–567.
41. B. Cox, *J. Nuclear Mater.,* 148 (1987), pp. 332–343.
42. B. Cox and Y. Yamaguchi, *J. Nuclear Mater.,* 210 (1994), pp. 303–317.
43. J.L. Bechade, R. Brenner, P. Goudeau, and M. Gailhanou, *Revue de Metallurgie, Cahiers D'Informations Techniques,* 100 (2003), pp. 1151–1156.
44. J.-L. Béchade, R. Brenner, P. Goudeau, and M. Gailhanou, *Mater. Sci. Forum,* 404-407 (2002), pp. 803–808.
45. N. Petigny, P. Barberis, C. Lemaignan, C. Valot, and M. Lallemant, *J. Nuclear Mater.,* 280 (2000), pp. 318–330.
46. J. Godlewski, P. Bouvier, G. Lucazeau, and L. Fayette, "Stress Distribution Measured by Raman Spectroscopy in Zirconia Films Formed by Oxidation of Zr-based Alloys," *Twelfth Int. Symp. Zr Nuclear Ind.,* ASTM STP 1354 (West Conshohocken, PA: ASTM, 2000), pp. 877–900.
47. P. Goudeau, D. Faurie, B. Girault, P.O. Renault, E. Le Bourhis, P. Villain, F. Badawi, O. Castelnau, R. Brenner, J.L. Bechade, G. Geandier, and N. Tamura, *Mater. Sci. Forum,* 524-525 (2006), pp. 735–740.
48. J. Godlewski, J.P. Gros, M. Lambertin, J.F. Wadier, and H. Weidinger, *9th Int. Symp. on Zr in the Nuclear Industry*, ASTM STP 1132 (West Conshohocken, PA: ASTM, 1991), pp. 416–436.
49. H. Li, H.M. Glavicic, and J.A. Spuznar, *Mater. Sci. and Eng.,* A366 (2004), pp. 164–174.
50. A. Motta, A. Yilmazbayhan, M. Gomes da Silva, R.J. Comstock, G. Was, J. Busby, E. Gartner, Q. Peng, Y.H. Jeong, and J.Y. Park, *J. Nuclear Mater.,* 371 (2007), pp. 61–75.
51. A.T. Motta and Y.H. Jeong, "Advanced Corrosion Resistant Zr Alloys for use in High Burnup and generation IV Systems," I-NERI Research Project # 2003-020-K (ROK-USA, 2003–2006), doi 10.2172/895014.

Arthur T. Motta is with the Department of Mechanical and Nuclear Engineering, Pennsylvania State University, University Park, PA 16802; atm2@psu.edu.